Numerical analysis of extended end-plate connections under dynamic loading

Djamel Aouiche[a] *, Noureddine Lahbari[b], Mourad Belhadj[b]
[a] The Department of Mechanical Engineering, University Batna 2 (Mostefa Ben Boulaïd), Batna 05000, Algeria
[b] The Department of Civil Engineering, University of Batna 2 (Fesdis), Batna 05078, Algeria
*Corresponding author: djamel.aouiche@univ-batna2.dz

Abstract

An experimental investigation was conducted at Delft University of Technology to examine the behavior of eight statically loaded extended end plate moment connections up to collapse. The parameters investigated were the end plate thickness (10 mm, 15 mm, and 20 mm) and steel grade of the end plate (S355, S690). While the study was limited to a static test, this investigation intends to analyze the dynamic behavior of the research specimens (FS1 to FS4) using finite element methods. The multi-purpose software Abaqus was used to develop the 3D model. The mechanical properties of these connections, including strength, ductility, and energy dissipation capacity, are examined. The cyclic loading is applied according to the JGJ 101-96 standard specification. The finite element model was validated against experimental tests for both static and dynamic conditions, successfully reproducing moment-rotation curves and simulating ductile damage as well. The results indicate that increased plate thickness corresponds to improved stiffness and strength, while the use of higher steel grades introduces a delayed yield point and may reduce ductility, which must be balanced to optimize performance considering specific design requirements and loading conditions. Our findings align with previous findings and underscore the need for a better understanding of joint behavior under dynamic loading for seismic design since the strain rate at which load is applied significantly affects the material properties, which can significantly affect the performance of blast-resistant structures.

Keywords

Extended end-plate connections, Dynamic behaviour, Abaqus software, Ductility, Stiffness, Strength, Dynamic

1. Introduction

Bolted end plate connections have gained increasing interest and adoption in steel frame construction due to their multiple advantages, such as ease of fabrication and erection, in addition to their effectiveness and cost. This connection exhibits close to rigid behavior when thick plates, stiffeners, and large bolts are used, but it may show semi-rigid behavior when the plates become thinner, stiffeners are eliminated, and smaller bolts are used. Thus, their behavior ranges from full restraint (rigid) to partial restraint (semi-rigid). This can also be observed when using high-strength materials that exhibit near-rigid behavior compared to more ductile materials. Properly designed, the connection can provide sufficient flexibility and a maximum energy dissipation capacity through a mechanism allowing balanced energy dissipation by the bolts and the end plate, minimizing the risk of failure caused by the brittle fracture of the joint at welds (Moncarz et al., 2001).

Despite several parameters that can also affect the behavior of connections, such as pretensioning bolts in end plate connections, this significantly enhances their performance (Noferesti and Gerami). (2023) finds that increasing bolt pretension levels improves cyclic behavior, moment capacity, energy absorption, initial rotational stiffness, and ductility of connections. Moreover, using a reduced beam section can enhance structure safety by focusing the energy dissipation on the reduced beam section; the stress concentrations are alleviated by the joint itself. This redistribution of stress away from the joint region can help reduce the likelihood of localized stress concentrations that could lead to premature failure. (Liang et al., 2021). Moreover, several studies have shown that loading conditions also significantly affect the response of structures.

Grimsmo et al. (2015) found that joints absorbed more energy and exhibited greater ductility before failing in dynamic tests compared to quasi-static tests. ElSabbagh et al. (2019) indicate that the moment capacity for a specimen subjected to cyclic loading is always smaller than that when the same specimen is subjected to monotonic loading by a value ranging from 4% to 26% and with an average value of about 16%. The rotation capacity for cyclic loading is also smaller than that for monotonic loading by an average value of about 40%. Therefore, designers have to be more cautious when designing structures subjected to high cyclic loads or located in severe seismic zones. Safety factors can be considered in the design of such structures. This suggests that joints may perform better under sudden, intense loads. As a result, static tests alone may not provide a comprehensive understanding of the behavior of joints.

Extensive experimental research has been conducted on the stability of steel frame structures, notably after the January 17, 1994, Northridge earthquake, which is the most damaging earthquake in the U.S. since 1926, to search for optimum parameters of connection components to obtain a better balance between the mechanical properties of joints such as flexibility, ductility, strength, and capacity of energy dissipation. The study herein focuses on the performance of bolted steel end plates using different thicknesses of end plates and different steel grades under dynamic loadings.

Extensive experimental research has been carried out to study the influence of the end plate on the behavior of bolted beam connections.

Tsai et al. (1990) found that achieving excellent performance in connections involves using larger and stronger bolts with thicker end plates. Thicker end plates enhance joint moment resistance, resist shear forces, and limit bolt-prying forces. Larger-diameter bolts contribute to increased ductility. Alternatively, connections with sufficient ductility can be designed using thinner end plates and larger-diameter bolts. The use of thicker end plates and larger bolts reduces stress concentration, ensures uniform force distribution, and minimizes the risk of bolt failures. Due to the high cost of such testing and the large lack of parameters intervening in the behavior of joints, alternative methods have been proposed to capture the behavior of joints as accurately as possible.

Gašić et al. (2021) conducted numerical and experimental research to investigate the effect of end plate thickness and rib on the performance of an extended one-sided stiffened bolted end-plate moment connection. They found that varying the thickness of the end plate and rib can optimize material costs while impacting joint strength. Thinner end plates may reduce joint strength but offer economic benefits through material savings. Thinner end plates can preserve joint ductility, requiring detailed behavior calculations. Thicker ribs and increased rib size improve joint stiffness and resistance, resulting in better performance. The thickness of the end plate significantly influences the joint strength.

Bursi and Jaspart (1998) propose a three-dimensional beam finite element assembly to model bolt behavior in a simplified manner. The element model is developed using the ABAQUS code to simulate the stiffness and strength characteristics of isolated extended end-plate steel connections. Throughout the research, the comparison between computed values from the finite element models and actual measurements is highlighted to demonstrate the effectiveness and accuracy of the proposed models. While the paper highlights the effectiveness and accuracy of the proposed finite element models, it does not extensively discuss the potential sources of error or uncertainties in the simulation process. The study simplifies the behavior of bolts in the model by using a three-dimensional beam finite element assembly. This simplification may not

fully capture the complex behavior of bolts in actual steel connections, potentially affecting the accuracy of the simulation results. The paper does not investigate the influence of varying parameters such as load conditions, material properties, or geometric configurations on the steel's behavior.

Maggi et al. (2005) conducted a parametric study on the behavior of bolted extended end plate connections using a finite element model. The study considered material nonlinearities, geometrical, discontinuities, and large displacements. The comparison between numerical and experimental data for moment-rotation curves, end plate displacements, and bolt forces showed satisfactory agreement. The study found that using phenomenological T-stub failure models is appropriate for calculating the flexural strength of the end plate. It also demonstrated how the interaction between the end plate and bolts affects the behavior of the connections. The results showed that failures related to the formation of yield lines in the plate or bolt tension failure were well defined. The study demonstrated the feasibility of using FE modeling to develop a parametric analysis of bolted end plate connections and refine current design approaches to improve the characterization of connection behavior.

Wang Shi et al. (2013) studied the seismic behavior of steel frame end-plate connections through numerical simulations using ABAQUS software. The paper introduces an efficient finite element method for end-plate connections under cyclic loading patterns, considering material and geometry nonlinearities. It verifies numerical simulations with quasi-static tests, providing a robust tool for further analysis. The equivalent plastic strain (PEEQ) is used as an index to predict relative fracture tendency in steel connections under cyclic loading. It is described as a cumulative variable and a monotonically increasing function, aiding in understanding local ductility and fracture tendencies.

However, the ductile damage to the steel frame structure is still a major challenge for researchers. The study by Lin et al. (2022) investigates the seismic behavior of high-strength steel extended end-plate connections using a finite element model developed in Abaqus. The model accurately simulates the bending deformation of the endplate and column flange, effectively capturing the gap phenomena among the bolt nuts, endplate, and column flange. The simulated hysteresis loops closely match experimental results, demonstrating stable energy dissipation and accurate reproduction of cyclic loading effects. While the model is validated for cyclic and seismic performance analysis, further research is recommended to predict connection failures, such as bolt fracture and end-plate cracking, by calibrating material failure models for high-strength steels and bolts.

This study examines the response of four extended end-plate connections (EEPC) specimens to dynamic loading conditions using Abaqus software. The specimens were previously tested under static loading by Coelho et al. (2004) at Delft University of Technology. The model developed herein can accurately capture the ductile damage of specimens as well, and the mechanical properties of joints are discussed based on the moment rotation curve plotted for each specimen. The results are discussed, and a conclusion is made about the influence of the end plate on the behavior of EECP.

2. Materials and Methods

2.1 Test setup and boundary conditions

Four distinct configurations of extended end plate connections are investigated. Two key parameters of the end plate are studied: the thickness (tp) and steel grade, as detailed in Table 1 (Coelho et al., 2001). M20 bolts of steel grade 8.8 were used to fasten the end plate to the column flange. Fig. 1 illustrates a typical setup configuration. In the initial step, a force of 450 KN was applied to the top of the column. The free end of the beam is restrained against rotation about the longitudinal axis to avoid any torsion or twisting. In addition, displacement along the lateral axis is restrained to avoid any movement out of plane. The column flange is retrained in all directions, including in the initial step. A bolt pretension force can be applied in a general static test; however, in a dynamic explicit step, this property is not available. Different levels of pretension bolt loads have been determined based on α times. 70% of the minimum tensile strength of bolts is based on ASC 360.lateral torsional buckling.

2.2 Loading procedure

The specimens are tested under static and dynamic loading in order to see the performance of joints under different conditions of loading. The procedure of loading is described below.

Static loading

A displacement control is applied to the end of the beam, where a displacement of 0.02 mm/s is applied to the extremity of the beam (Coelho et al., 2004). In Abaqus, the displacement is applied in a dynamic explicit step using a tubular table, with the amplitude incremented each second by 0.02 mm until the total displacement is reached as given by the

experimental results. The mass scaling of 1000 is used to increase the time calculation.
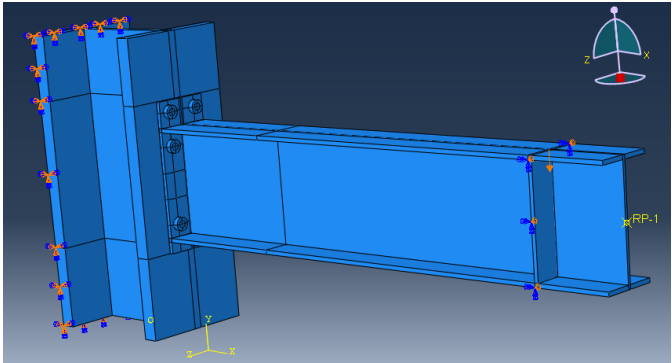

Fig. 1 Geometry of the specimens

Table 1. Details of the test specimens

Test ID	Column		Beam		End plate	
	Profile	Grade	Profile	Grade	tp (mm)	Grade
FS1	HE340M	S355	IPE300	S235	10	S355
FS2	HE340M	S355	IPE300	S235	15	S355
FS3	HE340M	S355	IPE300	S235	20	S355
FS4	HE340M	S355	IPE300	S235	10	S690

Cyclic loading protocol

The specimens were cyclically loaded following the JGJ 101-96 protocol established by the Ministry of Housing and Urban-Rural Development of the People's Republic of China. This protocol provides comprehensive guidelines for conducting cyclic loading tests, including load and displacement control stages. In the finite element, the load at the yielding point is applied in three steps. Then the procedure switches to displacement. Two cycles are applied, incrementing each step by 10 mm, as depicted in Fig. 2.

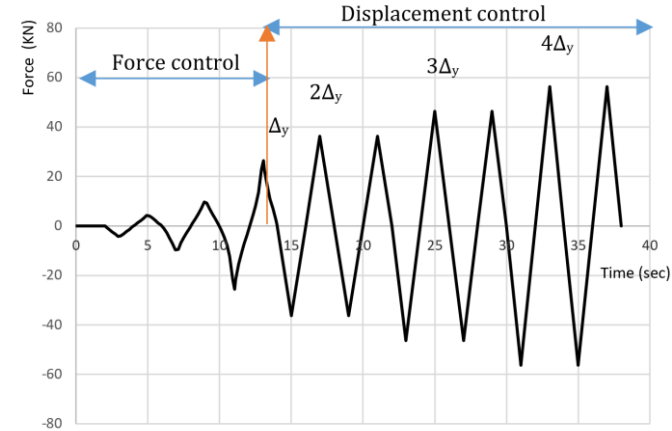*Fig. 2 JGJ 101-96 Cyclic loading protocol*

2.3 Contact definition

In finite element analysis, accurate contact definition is critical to reliably simulating complex structural interactions. The Abaqus software provides a complete set of tools for modeling contact interactions. Two main types of contact are implemented in Abaqus: normal contact and tangential contact, each of which uses specific algorithms. Tangential contact simulations are performed using slip or stick-slip methods. These methods consider frictional forces and constraints on relative motion between the contacting surfaces. Normal contact is modeled by the normal or gap penalty algorithms. These algorithms consider interactions that are perpendicular to the contacting surface. Moreover, the software uses a master-slave surface configuration to effectively capture complex interactions between components. In this approach, stiffer or larger surfaces are designated as master surfaces, while their more compliant or smaller counterparts serve as slave surfaces. For accurate results, it is critical to select appropriate contact algorithms and carefully define master-slave relationships. These methods allow the simulation of various contact conditions, including frictionless, frictional, bonded, and separation scenarios. Analysts can gain valuable insight into stress distributions, potential slip, and overall structural performance under both static and dynamic loading conditions in a wide range of engineering applications by carefully defining contact parameters.
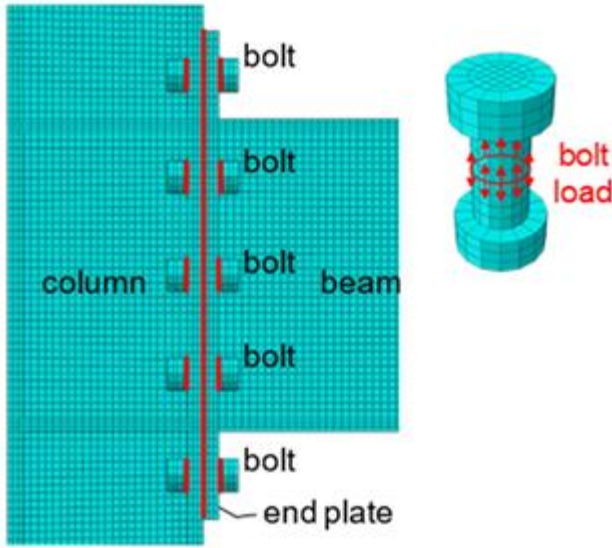
Fig. 3 Contact pairs and bolt load

2.4 Element types and meshes

The selection of element type and mesh configuration in Abaqus is crucial for obtaining reliable finite element analysis (FEA) outcomes. To accurately model incompressible materials and mitigate shear locking issues, the C3D8R (8-node linear brick, reduced integration, hourglass control) element was selected within the explicit element library. Additionally, the element deletion module was activated to account for material failures during the simulation.

However, it is important to note that this element can lead to increased computational costs due to its reduced integration scheme. Therefore, achieving an optimal balance between accuracy and computational efficiency is essential when determining the appropriate element type. In addition to the element type, the mesh configuration plays a critical role in achieving precise simulation results. The mesh density should be fine in critical zones to capture detailed material behavior, yet not excessively fine in other regions to avoid prohibitively long computation times. Furthermore, employing a uniform mesh distribution in critical areas is crucial to preventing biases in the simulation results caused by mesh irregularities. Fig. 4 illustrates the mesh results strategy.
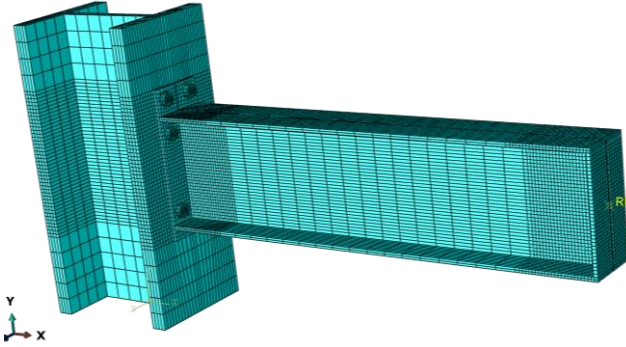

Fig. 4 Meshing technic using C3D8I element

2.5 Material Modelling

Under quasi-static loading

For initial analysis, the conventional engineering stress-strain relationship, as measured in the tensile coupon tested by Coelho et al. (2004), serves as a sufficient approach. It defines the axial force per unit initial area and the corresponding change in length per unit initial length. Fig. 5 shows the stress-strain curve for the material used in the test.

However, when modeling large strain behavior, this approach loses accuracy due to the changing cross-sectional area during deformation. To address this limitation, a true stress-strain approach is employed. The true strain ε_T and the true stress σ_T are defined with respect to the coupon's current length and cross-sectional area. They are related to conventional quantities by means of the following relationships:

$$\varepsilon_T = \ln(1 + \varepsilon_e) \tag{1}$$

$$\sigma_T = \sigma_e * (1 + \varepsilon_e) \tag{2}$$

To model the plastic behavior of a material in Abaqus, the elastic part must be subtracted from the total strain, resulting in a plastic strain (ε_p) equal to:

$$\varepsilon_p = \varepsilon - \varepsilon_e = \varepsilon_e - \frac{\sigma}{E} \tag{3}$$

where ε is total strain, ε_e is elastic strain, σ is stress, and E is the elastic modulus.
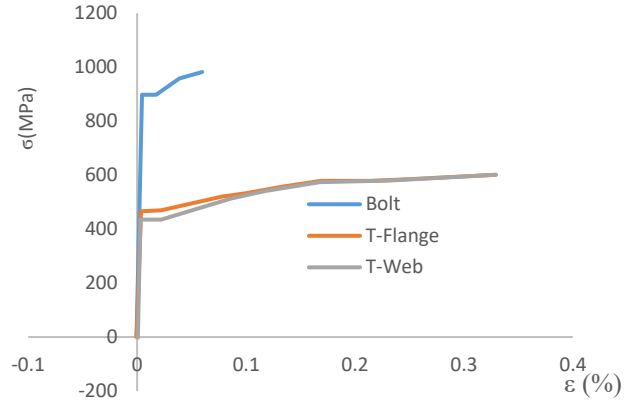

Fig. 5 Stress strain curve materials

Material modelling under dynamic loading

The Chaboche nonlinear isotropic/kinematic hardening model (Chaboche, J. L.,1986,1989) is used for the simulation of the Von Mises flow rule of steel under cyclic loading. Isotropic hardening describes the evolution of the yield surface size. $\sigma|0$ is a function of the equivalent plastic strain and is expressed as a simple exponential law. $\sigma|0$ is the initial yield stress at zero plastic strain, while $Q\infty$ and b are material parameters. $Q\infty$ is the maximum change in the size of the yield surface, and b defines the rate at which the size of the yield surface changes as plastic strain develops. The parameters of S355 steel for use in ABAQUS are given in Table 2 (Krolo & Grandic, 2021).

Table 2. Calibration parameters of S355 steel.

$\sigma|0$	$Q\infty$	b	$C1$	$\gamma1$	$C2$	$\gamma2$	$C3$	$\gamma3$
386	20.8	3.2	5327	75	1725	16	1120	10

2.6 Implementation of ductile damage model in Abaqus

The implementation of ductile damage models in Abaqus results in a more accurate simulation of material behavior up to and including failure. This is especially crucial in structural engineering applications, where considering the full range of material responses, including post-yield behavior, is critical. When implementing the ductile damage model, meticulous calibration of the damage parameters is paramount. This often involves comparing simulation results with experimental data and adjusting the parameters iteratively to achieve agreement.

The presence of void nucleation, growth, and coalescence mechanisms typically characterize ductile fractures, indicating significant plastic deformation prior to failure. The implementation of ductile damage in Abaqus requires the use of a curve that relates the deformation at the beginning of the fracture with the triaxial stress. The modeling of the material for the damage requires the definition of four parameters, which are presented below and whose points are outlined in Fig. 6. The dashed green curve is idealized assuming no damage occurs, whereas the blue solid line corresponds to the real state where damage occurs. σ_{yo} and $\bar{\varepsilon}_0^{pl}$ are the ultimate strength and equivalent plastic strain at the onset of damage, while $\bar{\varepsilon}_f^{pl}$ is the equivalent plastic strain at failure
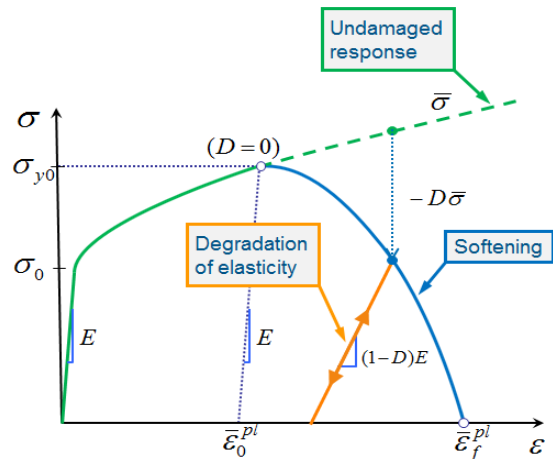

Fig. 6 Stress-strain curves with progressive damage degradation

The onset of damage and damage evolution can be predicted following the principal formulation proposed by to (Hooputra et al., 2004), which is included in the ABAQUS 6.14 software package. The model assumes that a ductile metal can break in two main ways: i) ductile fracture caused by nucleation, growth, and coalescence voids; and ii) shear fracture caused by shear band localization. In this paper, only the model for ductile fracture is implemented; it assumes that the equivalent plastic strain at the beginning of damage $\overline{\varepsilon}_0^{pl}$ is dependent on the strain rate and stress triaxiality, defined by ($\sigma H/ \sigma eq$), where σH is the hydro static pressure stress (isotropic stress) and σeq is the equivalent von Mises stress (equation 4).

$$\sigma_e = \sqrt{\begin{array}{c} \frac{1}{2}((\sigma_{11} - \sigma_{22})^2 + (\sigma_{33} - \sigma_{22})^2 \\ + (\sigma_{11} - \sigma_{33})^2 + 6\tau_{12}^2 + 6\tau_{13}^2 + 6\tau_{23}^2 \end{array}} \quad (4)$$

The damage evolution description based on linear displacement is used; it requires the definition of the effective plastic displacement $\overline{u}^{pl} = L. \overline{\varepsilon}_f^{pl}$

where $\overline{\varepsilon}_f^{pl}$ the equivalent plastic strain at failure and L is the characteristic length of the finite element.

Due to the strain localization during the progressive damage, the response is mesh dependent. As elements reach a user-defined level of degradation (for instance, the maximum degradation corresponds to $D = 1$) following $\sigma = (1 - D)$, elements may be either kept or removed from the mesh. Ductile damage parameters for S355 used herein to model the end plate in FS1 to simulate the moment rotation curve until failure and mode of failure are given in Table 3 and Table 4 for both quasi-static and dynamic cases (Krolo & Grandic, 2021).

Table 3. Parameters of damage model for S355 (cyclic loading).

Damage Initiation Criteria			Damage Evaluation Low	
$\overline{\varepsilon}_D^{pl}$	η	$\dot{\varepsilon}^{pl}$	D	$\overline{u}_i^{pl}$
0.6308	0.33	0.001	0	0
0.62491	0.38	0.001	0.0085	0.4719
0.61874	0.43	0.001	0.0243	0.9666
0.61244	0.48	0.001	0.0623	1.4716
0.60607	0.52	0.001	0.1293	1.9823
0.59963	0.57	0.001	0.2386	2.4987
0.5931	0.61	0.001	1	3.022

Table 4. Parameters of damage model for S355 (monotonic loading).

Damage Initiation Criteria			Damage Evaluation Low	
$\overline{\varepsilon}_D^{pl}$	η	$\dot{\varepsilon}^{pl}$	D	$\overline{u}_i^{pl}$
0.2270	0.32	0.001	0	0
0.2070	0.50	0.001	0.0105	0.0580
0.1945	0.60	0.001	0.0305	0.0965
0.1822	0.70	0.001	0.0625	0.1346
0.1755	0.76	0.001	0.0872	0.1562
0.1676	0.82	0.001	0.1183	0.1788
0.1562	0.90	0.001	0.1701	0.2087

2.7   Validation of the model under cyclic loading

The specimen JD1 (Shi et al. 2007), as depicted in Fig. 7, is used to verify the accuracy of the finite element model. The author conducted a study on the behavior of end-plate moment connections on steel beam-to-column connections under cyclic loads. The study examined various parameters such as end-plate thickness, bolt diameter, endplate extended stiffener, column stiffener, and type of flush and extended endplate. All components are made from Q345 steel, except for the bolts, which are 10.9 steel grade. For a detailed description of the material properties used, see Wang Shi et al. (2013). The ductile damage parameters for S355 are given in tables 6 and 7. These can be used since Q345 and S355 are equivalent in terms of mechanical properties. The cyclic loading procedure was a force/displacement control method according to the JGJ 101-96 specification for seismic testing.

The results of these tests, as depicted in Fig. 8, demonstrate a favorable agreement between the model's predictions and the experimental observations.
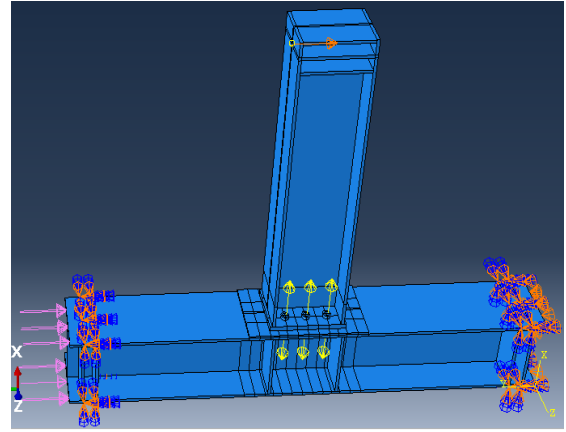

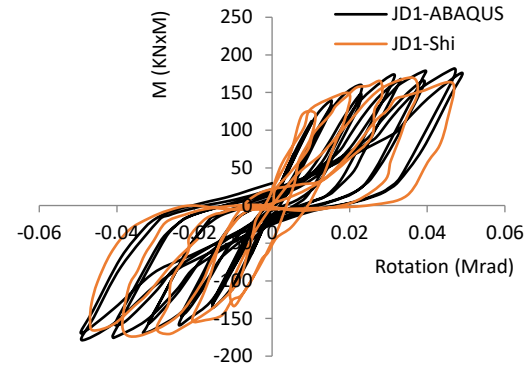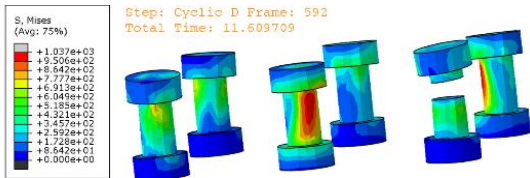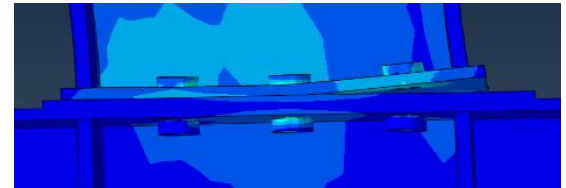**Fig. 7 Setup configuration and boundary condition JD1**

Fig. 8 Moment rotation curve-JD1 Abaqus-Shi

(a) Failure in bolt of JD1 specimens numerical results

(b) Failure in bolt of JD1 specimens' experimental results

Fig. 9 Failure in bolt of JD1

2.8   Test procedure

The investigation involves two stages:
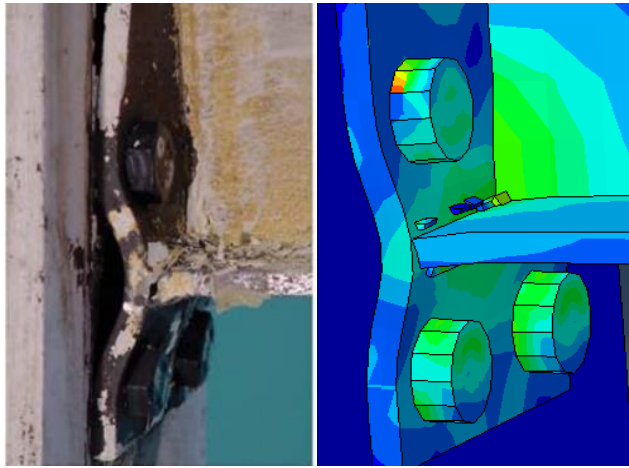
Static loading

Specimen FS1 was examined under static loading conditions up to collapse using finite element modeling (FEM).
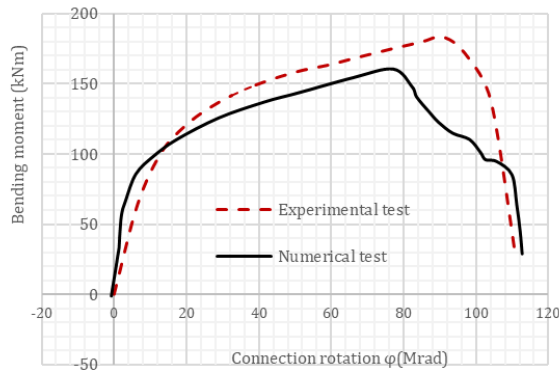
Dynamic loading

All specimens (FS1, FS2, FS3, and FS4) are then analyzed under dynamic loading using FEM. According to the JGJ 101-96 cyclic loading protocol, as illustrated in Fig. 2. The moment-rotation curve's hysteresis loop is plotted for each specimen. These plots are used to assess the specimens' response to repetitive loads, providing insight into their dynamic behavior and energy dissipation characteristics

3. Results

The simulation results for the specimen FS1 under static loading up to collapse are presented in Fig. 10, showing the weld failure mode compared to experimental observations as illustrated in Fig. 10 (a) and comparing the moment-rotation data between FEM and experimental results as depicted in Fig. 10 (b). Fig. 11 presents the hysteresis loop of the moment rotation curve obtained using the numerical model for all specimens (FS1, FS2, FS3, and FS4) under cyclic loading, presenting These findings demonstrate the FEM's capability in capturing both static and dynamic behaviors of the connections, providing a foundation for further analysis and validation of the model's accuracy and robustness.

(a) mode failure

(b) moment-rotation up to failure in FSS

Fig. 10 ductile damage in specimen FS1 under static loading

4. Discussion

The study reveals significant differences between static and dynamic responses of extended end-plate connections. Dynamic loading generally resulted in higher moment capacities across all specimens compared to static loading. This finding underscores the importance of considering dynamic effects in connection design, particularly for seismic applications. Static tests alone may underestimate the connection strength in dynamic situations, potentially leading to overly conservative designs.

End Plate Thickness:

The results confirm that increasing end plate thickness improves connection stiffness and strength under both static and dynamic loading. However, the difference between static and dynamic responses was more pronounced for thinner plates (FS1) compared to thicker ones (FS2 and FS3). This suggests that the benefits of increased thickness may be more significant in dynamic loading scenarios, particularly for more flexible connections.

Steel Grade:

The use of higher strength steel (S690 in FS4 vs S355 in FS1) resulted in increased moment capacity under both static and dynamic loading. However, the higher strength steel also exhibited a slightly more brittle response with less rotation capacity before failure. This trade-off between strength and ductility is crucial for designers to consider, especially in seismic design where both high strength and ductility are desirable.

Energy Dissipation:

The hysteresis loops obtained from dynamic loading provide valuable information on the energy dissipation capacity of the connections. This data, not available from static tests, is crucial for understanding how connections will perform under repeated cyclic loading during seismic events.

Ductile Damage Modeling:

The ability of the finite element model to capture ductile damage provides insights into potential failure modes under dynamic loading. This capability enhances our understanding of connection behavior beyond what can be observed in static tests or simulations without damage modeling.

Validation of FEA Approach:

The study demonstrates the effectiveness of finite element analysis in modeling both static and dynamic behavior of extended end-plate connections. The good agreement between numerical results and experimental data validates this approach for future parametric studies.
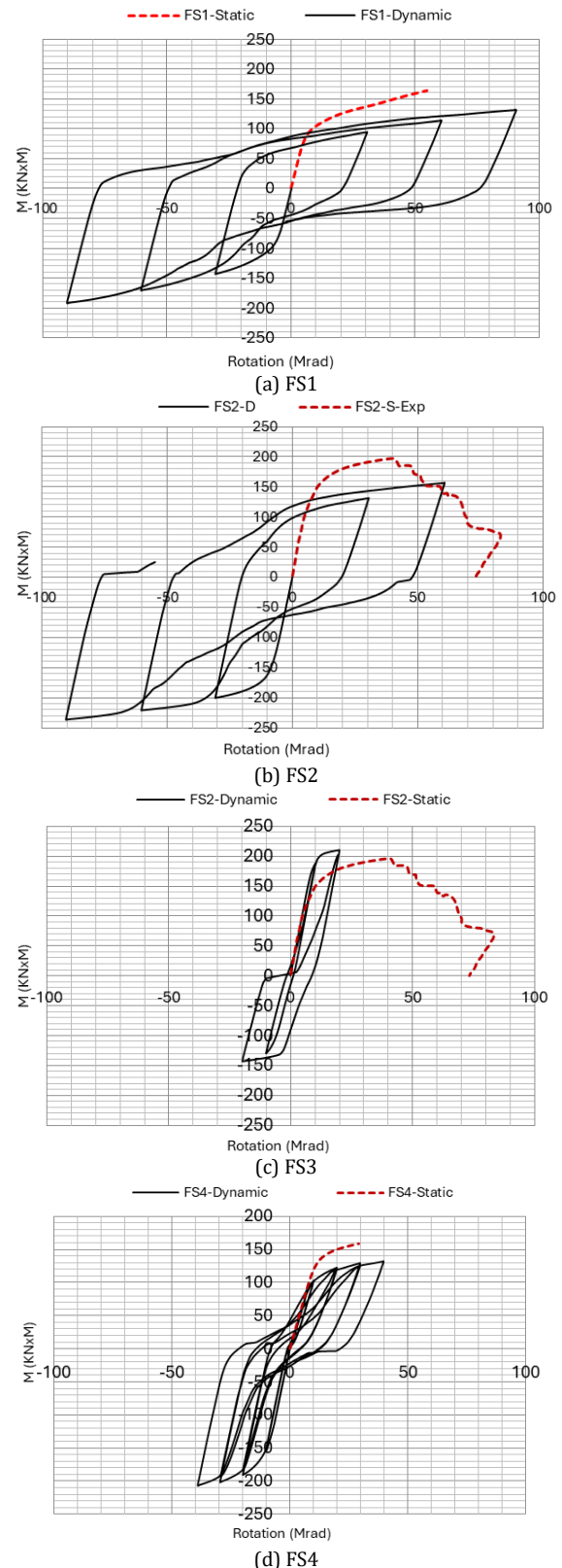

(a) FS1

(b) FS2

(c) FS3

(d) FS4

Fig. 11 Moment -rotation of joint under cyclic loading

5. Conclusion

This research explores the behavior of extended end-plate connections under dynamic loading conditions. It reveals that dynamic loading generally results in higher moment capacities than static loading, suggesting that static tests might underestimate the true strength of connections.

The study also highlights the influence of end plate thickness and steel grade on connection performance. Increasing the end plate thickness enhances the stiffness and strength of the joint, while using higher-grade steel can delay yielding but may reduce ductility. Balancing stiffness, strength, and ductility to optimize joint performance according to design requirements should be carefully considered.

The differences between static and dynamic responses are more pronounced in more flexible connections, underscoring the necessity for dynamic analysis.

Finite element analysis, including ductile damage modeling, proves effective in simulating complex connection behavior under different loading conditions.

The findings have significant implications for seismic design, suggesting that current design practices that rely primarily on static analysis may be overly conservative and undervalue ductility and energy dissipation capacity.

Future research should expand the range of parameters studied and include experimental validation of dynamic loading results. Overall, this research provides valuable insights into structural engineering, particularly in the design of connections under dynamic loading conditions, emphasizing the importance of considering both static and dynamic behaviors in the design process.

References

AISC 360, Specifcations for Structural Steel Buildings,American Institute of Steel Construction, Chicago, IL, USA,2016. https://www.aisc.org/globalassets/aisc/publications/standards/a360-16-spec-and-commentary_june-2018.pdf

Bursi, O. S., & Jaspart, J. P. (1998). Basic issues in the finite element simulation of extended end plate connections. Computers & structures, 69(3), 361-382. https://doi.org/10.1016/S0045-7949(98)00136-9

CEN, E. (2005). 3: Design of steel structures, Part 1.8: Design of joints. Brussels: European Committee for Standardization. https://www.phd.eng.br/wpcontent/uploads/2015/12/en.1993.1.8.2005-1.pdf

Chaboche JL. Constitutive equations for cyclic plasticity and cyclic viscoplasticity. Int J Plast 1989;5(3):247–302. https://doi.org/10.1016/0749-6419(89)90015-6

Chaboche JL. Time independent constitutive theories for cyclic plasticity. Int J Plast1986;2(2):149–88. https://doi.org/10.1016/0749-6419(86)90010-0

Coelho, A. M. G., Bijlaard, F. S., Gresnigt, N., & da Silva, L. S. (2004). Experimental assessment of the behavior of bolted T-stub connections made up of welded plates. Journal of constructional Steel research, 60(2), 269-311. https://doi.org/10.1016/j.jcsr.2003.08.008

ElSabbagh, A., Sharaf, T., Nagy, S., & ElGhandour, M. (2019). Behavior of extended endplate bolted connections subjected to monotonic and cyclic loads. Engineering Structures, 190, 142-159. https://doi.org/10.1016/j.engstruct.2019.04.016

Gašić, V., Arsić, A., & Zrnić, N. (2021, October). Strength of extended stiffened endplate bolted joints: Experimental and numerical analysis. In Structures (Vol. 33, pp. 77-89). Elsevier. https://doi.org/10.1016/j.istruc.2021.04.016

Grimsmo, E. L., Clausen, A. H., Langseth, M., & Aalberg, A. (2015). An experimental study of static and dynamic behaviour of bolted end-plate joints of steel. International Journal of Impact https://doi.org/10.1016/j.ijimpeng.2015.07.001

Hooputra H, Gese H, Dell H, Werner H (2004) A comprehensive failure model for crashworthiness simulation of aluminium extrusions. Int J Crash 9:449–463 https://doi.org/10.1533/ijcr.2004.0289

JGJ 101-1996: Specification of testing methods for earthquake resistant building, Architecture & Building Press, Beijing, China, 1996. in Chinese. https://www.chinesestandard.net/PDF/English.aspx/JGJ101-1996

Krolo, P., & Grandić, D. (2021). Hysteresis envelope model of double extended endplate bolted beam-to-column joint. Buildings, 11(11), 517. https://www.mdpi.com/2075-5309/11/11/517

Liang, G., Lu, Z., Guo, H., Liu, Y., Yang, D., Li, S., & Pan, X. (2021). Experimental and numerical investigation on seismic performance of extended stiffened end-plate joints with reduced beam section using high strength steel. Thin-Walled Structures, 169, 108434. https://doi.org/10.1016/j.tws.2021.108434

Lin, T., Wang, Z., Hu, F., & Wang, P. (2022). Finite-element analysis of high-strength steel extended end-plate connections under cyclic loading. Materials, 15(8), 2912. https://www.mdpi.com/1996-1944/15/8/2912

Lin, T., Wang, Z., Hu, F., & Wang, P. (2022). Finite-element analysis of high-strength steel extended end-plate connections under cyclic loading. Materials, 15(8), 2912. 10.3390 /ma15082912

Maggi, Y. I., Gonçalves, R. M., Leon, R. T., & Ribeiro, L. F. L. (2005). Parametric analysis of steel bolted end plate connections using finite element modeling. Journal of Constructional Steel Research, 61(5), 689-708. https://doi.org/10.1016/j.jcsr.2004.12.001

Moncarz, P. D., McDonald, B. M., & Caligiuri, R. D. (2001). Earthquake failures of welded building connections. International journal of solids and structures, 38(10-13), 2025-2032. https://doi.org/10.1016/S0020-7683(00)00150-5!

Noferesti, H., & Gerami, M. (2023). Cyclic Behavior of Bolted Stiffened End-Plate Moment Connections for Different Bolt Pretensioning Levels: An Experimental Study. Shock and Vibration, 2023(1), 5330905. https://doi.org/10.1155/2023/5330905

Shi, G., Shi, Y., & Wang, Y. (2007). Behaviour of end-plate moment connections under earthquake loading. Engineering structures, 29(5), 703-716. https://doi.org/10.1016/j.engstruct.2006.06.016

Tsai, K. C., Wu, S., & Popov, E. P. (1995). Experimental performance of seismic steel beam-column moment joints. Journal of Structural Engineering, 121(6), 925-931. https://doi.org/10.1061/(ASCE)0733-9445(1995)121:6(925)

Wang, M., Shi, Y., Wang, Y., & Shi, G. (2013). Numerical study on seismic behaviors of steel frame end-plate connections. Journal of Constructional Steel Research, 90, 140-152. https://doi.org/10.1016/j.jcsr.2013.07.033!